Materials Characterization 121 (2016) 187–194

Contents lists available at ScienceDirect

Materials Characterization

journal homepage: www.elsevier.com/locate/matchar

Microstructure and mechanical properties of friction stir processed Cu with an ideal ultrafine-grained structure

P. Xue [a], B.B. Wang [b], F.F. Chen [a], W.G. Wang [b], B.L. Xiao [a], Z.Y. Ma [a,*]

[a] Shenyang National Laboratory for Materials Science, Institute of Metal Research, Chinese Academy of Sciences, 72 Wenhua Road, Shenyang 110016, China
[b] School of Mechanical Engineering, Liaoning Shihua University, 1 West Dandong Road, Fushun 113001, China

ARTICLE INFO

Article history:
Received 1 September 2016
Received in revised form 7 October 2016
Accepted 8 October 2016
Available online 11 October 2016

Keywords:
Friction stir processing
Ultrafine-grained structure
Pure copper
Microstructure
Strength
Ductility

ABSTRACT

Ultrafine-grained (UFG) Cu with uniform microstructure was successfully prepared by friction stir processing (FSP) under additional water cooling. FSP Cu exhibited equiaxed grains with low dislocation density, weak texture, and high fraction of high-angle grain boundaries. Isotropy and tension-compression symmetry were achieved in FSP Cu sample, which provided an ideal model material to investigate the intrinsic mechanical behavior of the UFG material. Enhanced strain hardening was achieved in FSP Cu due to the special microstructure which was effective in accumulating dislocations, resulting in good strength-ductility synergy. This study provides a feasible strategy of preparing bulk UFG materials with good mechanical properties.

1. Introduction

Ultrafine-grained (UFG) materials have attracted extensive concern due to their significantly enhanced hardness and strength [1]. However, most of these materials have low tensile ductility at ambient temperature, which limits their practical applications. The elongation to failure is far less than that of their coarse-grained (CG) counterpart [2,3]. Usually, the disappointingly low ductility can be attributed to the artifacts from processing, the plastic instability (necking or shear localization) with little or no strain hardening (dislocation storage) capacity, and low resistance to crack initiation and propagation [4].

One-step severe plastic deformation (SPD) methods, such as equal-channel angular pressing (ECAP), high-pressure torsion (HPT) and dynamic plastic deformation (DPD), provide practical approaches to producing bulk UFG materials that can exhibit mechanical properties controlled by their intrinsic deformation mechanisms [1,3]. Usually, unstable microstructure with high density of dislocations and strong texture is obtained in SPD UFG materials, which results in insufficient strain hardening capacity [4,5]. Plastic instabilities in such non-equilibrium systems of heavily deformed metals are very common and have been proven to occur, and low tensile ductility is still achieved in these UFG materials [6]. Moreover, grain coarsening and large-scale shear bands are easily formed during cyclic deformation, which are very harmful to the fatigue properties of the UFG materials [7]. Therefore, new methods are expected to be produced in order to improving the mechanical properties of the UFG materials.

Based on the principle of friction stir welding (FSW), Mishra et al. [8] developed a new SPD method of friction stir processing (FSP) for microstructural modification of materials. FSP has been shown as an effective technique in many applications, such as refining the microstructure of cast alloys, fabricating surface composites, and producing fine-grained structure, which exhibits good superplasticity [9,10]. Recently, FSP has been proven to be an effective method to prepare bulk UFG materials, such as Al, Mg, Cu, Ni and their alloys [11–18].

The grain refinement mechanism of FSP is dynamic recrystallization (DRX), so fine and equiaxed grains with quite uniform sizes are produced in the processed zone (PZ) [9–19]. Usually, SPD UFG materials exhibit high density of dislocations and most grain boundaries (GBs) are wavy, diffuse, and ill-defined non-equilibrium GBs [4,20]. Differently, large fraction of equilibrium high-angle grain boundaries (HAGBs, misorientation angle ≥15°) are obtained in the FSP UFG materials, and low density of dislocations exist in the ultrafine grains. Therefore, good strength and ductility can be obtained in the FSP UFG materials compared to that of other SPD materials, resulting from the enhanced strain hardening [11–19]. In this study, UFG materials were successfully prepared by FSP with additional water cooling in pure Cu samples, and the microstructure and mechanical properties of the FSP Cu were investigated and the strength-ductility relationships of various UFG Cu samples were discussed.

* Corresponding author.
E-mail address: zyma@imr.ac.cn (Z.Y. Ma).

http://dx.doi.org/10.1016/j.matchar.2016.10.009
1044-5803/

2. Experimental Procedures

In order to compare with other findings of UFG Cu more accurately, we used two base materials (BM) with different purities: one is the common commercially pure Cu T3 (99.9%) and the other is high purity oxygen free Cu TU1 (99.99%). The schematic illustration of FSP process is shown in Fig. 1. Before FSP, the initial Cu plates were annealed at 700 °C for 2 h, and the grain size was about 200 μm. To yield low heat-input during FSP, the Cu plates were first fixed in water and additional cooling by flowing water was adopted. Detailed parameters about the water cooling have been stated in the previous study [21]. FSP process was performed on the Cu plates using a rotating tool with the shoulder 20 mm, 12 mm and 10 mm in diameter at relatively low rotation rates of 400 rpm, 600 rpm and 400 rpm, respectively. The FSP samples prepared by the above parameters were designated as FSP-T3-a, FSP-T3-b, FSP-T3-c and FSP-TU1-a, FSP-TU1-b, FSP-TU1-c for the T3 Cu and TU1 Cu samples, respectively.

Microstructural examination was completed with optical microscopy (OM), scanning electron microscope (SEM) equipped with electron backscatter diffraction (EBSD) system, and transmission electron microscopy (TEM). EBSD experiments were performed using an Oxford HKL Channel 5 system on a LEO Supra 35 FEG SEM with step size of 70 nm. In order to investigate the microstructural uniformity in the PZ, EBSD scans were performed in various areas of FSP T3 Cu samples. TEM observation was carried out on a FEI Tecnai G^2 20 microscope operating at 200 kV. Thin foils for TEM were twin-jet electropolished by a solution of 25% alcohol, 25% phosphorus acid and 50% deionized water at 263 K.

Micohardness tests were performed on the cross-section (*x*-*z* plane in Fig. 1) of FSP Cu samples, five points were tested on each specimen (the test positions were shown as the squares in Fig. 2), and the relationship between the grain size and hardness value was discussed. Moreover, in order to investigate the homogeneity of the mechanical properties in FSP UFG Cu, the hardness distribution in the PZ was tested in FSP-TU1-b sample. During the hardness test, a load of 50 g with a holding time of 15 s was used. For the tensile test, the dog-bone-shaped specimens with a gauge length of 5 mm and a width of 1.4 mm were machined along the processing direction from the PZ, and polished to a thickness of 0.7 mm. Meanwhile, we investigated the tensile and compression behaviors in different directions in the PZ of FSP-T3-a sample, i.e., perpendicular and parallel to the processing direction, respectively (*x* (transverse) and *y* (longitudinal) directions in Fig. 1). Uniaxial tensile tests were conducted at room temperature at an initial strain rate of $1 \times 10^{-3}\ s^{-1}$. For the compression test, the gauge length of the specimen is 4 mm and the size of cross section is 2 × 2 mm.

3. Results and Discussion

Fig. 2 shows the typical cross-sectional macrograph of the FSP Cu for FSP-TU1-b sample. A typical basin-shaped PZ which widened near the upper surface was observed on the transverse section of the FSP Cu,

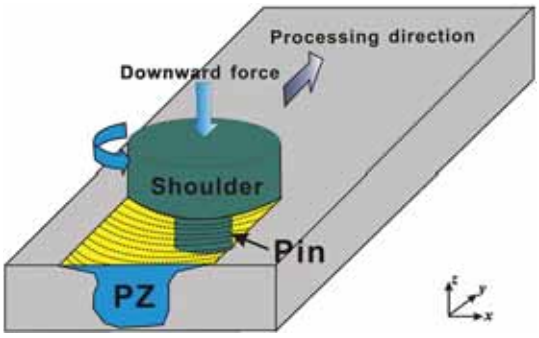

Fig. 1. Schematic illustration of FSP process.

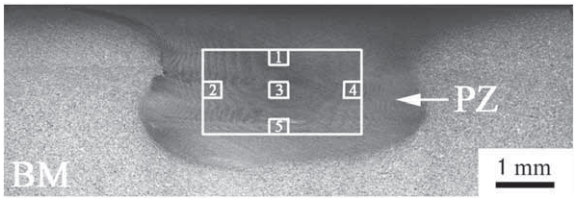

Fig. 2. Cross-sectional macrostructure and schematic positions for hardness test of processed zone (PZ).

and obvious onion rings could be observed which was similar to other observations in various studies [9,22,23].

Fig. 3 shows the EBSD microstructure at different positions of every 1.2 mm along the centerline of transverse sectioned PZ for FSP-T3-a sample. As can be seen from Fig. 3, all the EBSD micrographs in the PZ exhibited equiaxed grains, and the same average grain size and distribution characteristic were achieved in each area. Simultaneously, the microstructure of FSP-T3-b sample of every 120 μm along the vertical centerline from top to bottom in the PZ was analyzed by EBSD, as shown in Fig. 4. Similarly, the microstructure of each area from top to bottom in the PZ was almost the same, which also exhibited equiaxed grains with smaller grain size than that of the FSP-T3-a sample. Clearly, the microstructure was almost the same in every position of the whole PZ. Therefore, FSP is an effective method to prepare bulk UFG materials with uniform microstructure.

The typical TEM microstructure of FSP-T3-a, FSP-T3-b, FSP-TU1-b, and FSP-TU1-c samples is shown in Fig. 5. As can be seen from the TEM microstructure, the grains of FSP Cu exhibited equiaxed recrystallized state, and the dislocation density was low. Thus, the ultrafine grains obtained in FSP Cu under forced cooling were similar to those of the recrystallized grains in the nugget zone/PZ of conventional FSW/FSP processes, and DRX should be the main grain refinement mechanism in the present FSP Cu [9].

Moreover, as we can see from the TEM microstructure of the FSP Cu, under a same parameter (such as the b parameter), grain refinement was more notable in T3 Cu than that of TU1 Cu, as shown in Fig. 5b and c. The average grain sizes (containing sub-grains) of FSP-T3-b and FSP-TU1-b samples were about 500 nm and 800 nm, respectively (Table 1). It means that the presence of a small amount of impurity particles in T3 Cu provide more nucleation sites during recrystallization, which can effectively prevent the grain growth, resulting in the smaller grain size than that of the TU1 Cu.

However, the microstructure of FSP-TU1-b sample was similar to that of FSP-T3-a sample, and the average grain size was about 800 nm. Further, the microstructure of FSP-TU1-c sample was similar to that of FSP-T3-b sample, and the average grain size was about 500 nm. It is clear that approximately same microstructure was achieved in T3 Cu and TU1 Cu samples under different FSP parameters, and it is significant to investigate the mechanical behaviors of various UFG Cu samples.

Plenty of individual straight boundaries that traversed the whole grains were frequently observed in the ultrafine grains, as illustrated by the arrows in Fig. 5. According to the typical selected-area electron diffraction pattern shown in the upper right corner of Fig. 6a, most of these straight boundaries were Σ3 coincident-site lattice (CSL) twin boundaries (TBs) and exhibited the typical twin relationship of {111}/[112] type in Cu. These TBs should be annealing TBs which formed during the recrystallization process, according to the previous studies [15,24,25]. Moreover, from the typical high-resolution TEM image in Fig. 6b, it can be seen that these annealing TBs were perfectly coherent and no lattice dislocation was detected. These annealing TBs in FSP Cu were different from the deformation TBs in SPD Cu where excessive dislocations existed [4,20].

The TEM microstructural characteristics were further confirmed by EBSD studies in FSP-T3-a sample, as shown in Fig. 7. Similar to the TEM observations, the microstructure of FSP Cu was characterized by

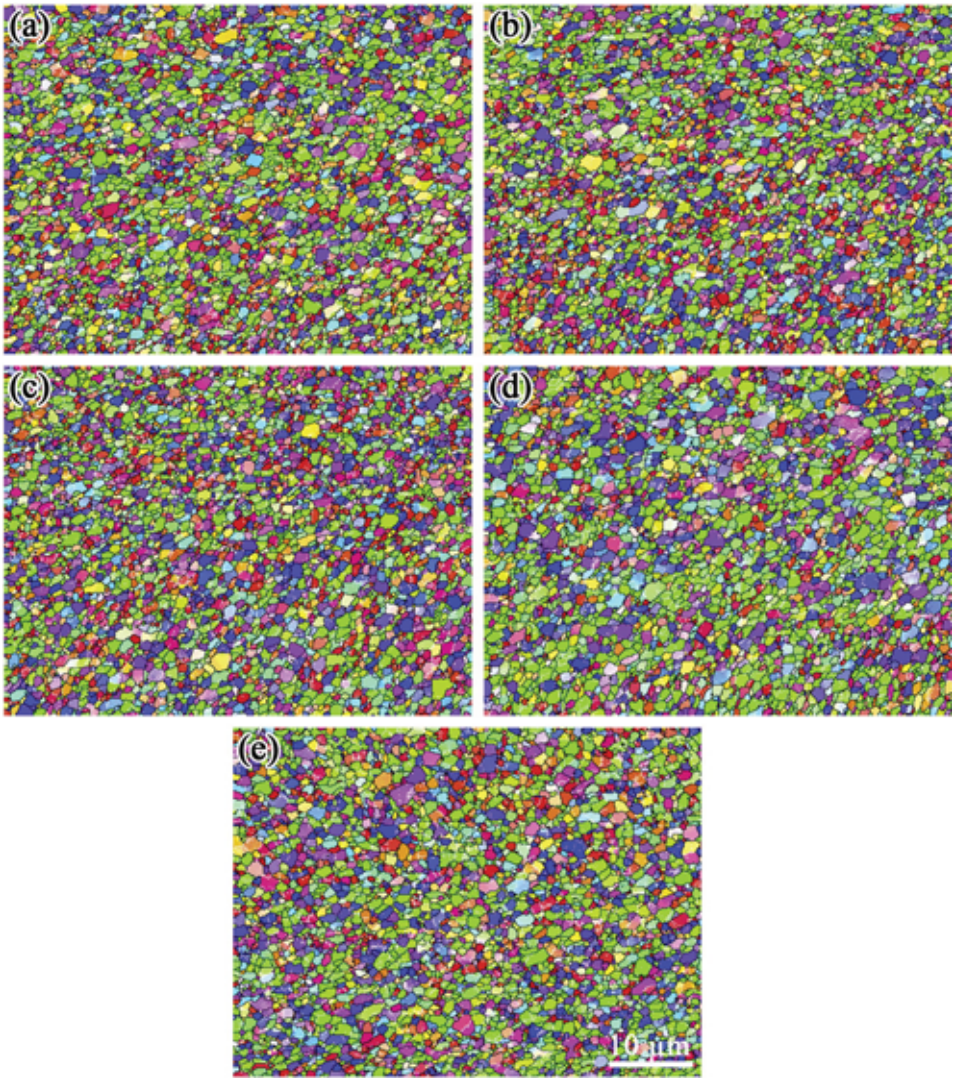

Fig. 3. EBSD microstructure of FSP-T3-a sample in the PZ (a–e: from left to right, along *x* direction in Fig. 1 with an interval of 1.2 mm).

fine grains with a typical equiaxed recrystallized microstructure (Fig. 7a). Fig. 7b shows the distribution map of the GB misorientation angle, it is clear that the misorientation angle distribution of FSP Cu was similar to that of the random distribution for a cubic polycrystalline. Considering all GBs with misorientation angles >2°, the HAGBs comprised about 91.5% of the total GB length, which was similar to that of FSP-TU1-b sample (~90%) [24]. Obviously, the fractions of HAGB in FSP Cu sample was larger than that in SPD Cu sample in which the fraction of HAGB reached only ~60% even after complex procedures [26].

From the distribution map of the GB misorientation angle for FSP Cu, a peak appeared at approximately 60° compared to that of the random distribution, which results from the Σ3 CSL TBs [15,24,25]. Fig. 7c shows a typical distribution map of Σ3 TBs in FSP-T3-a sample, and the red line represents the Σ3 TB. It is clear that these TBs were single TBs crossing the whole grain, and it was mainly distributed in the fine grains, which was similar to that of the TEM observation. In fact, the CSL GBs with low energy are very common in recrystallized structure. In addition to Σ3 TBs, other CSL GBs also existed in FSP Cu sample, as shown in Fig. 7d.

Moreover, similar to the conventional nugget zone/PZ in FSW/FSP samples, the texture of FSP Cu was very weak, and the maximum pole density was only 3 in FSP-T3-a sample from the pole figures in Fig. 7e. This further demonstrated that the grain refinement in FSP Cu was still a DRX mechanism. However, other UFG microstructure prepared by SPD process usually exhibited a strong texture. For example, the UFG Cu produced by ECAP showed an obvious shear texture due to strong shear plastic deformation [3–7].

In the earlier reports, many researchers demonstrated that the deformation TBs, with high density of dislocation and excess energy, were extensively exist in the UFG materials produced via SPD methods, so the feeble dislocation storage capacity limited the increase of ductility [4]. However, compared to deformation TBs, there are enormous differences in coherent TBs, which performed higher thermal and mechanical stability owing to the high capacity of dislocations accommodation [25]. In our present research, the TBs in the FSP UFG Cu samples were coherent annealing TBs, which tended to distribute in the finer grains and restrained the growth of grains [24].

The above microstructural analysis indicates that the microstructure of FSP Cu is very uniform in the whole PZ. Therefore, the mechanical properties of each area should be relatively uniform. From the hardness distribution map of FSP-TU1-b sample in the PZ, the differences of hardness values were very small in various areas, as shown in Fig. 8. Clearly, FSP Cu can be regarded as a uniform UFG material to investigate the intrinsic mechanical properties.

Fig. 9 shows the relationship between the hardness and grain size of FSP-TU1 Cu for different parameters in Table 1. In Fig. 9, the solid line was the fitted Hall-Petch line of CG Cu and two dotted lines represented the upper and lower boundaries to meet the Hall-Petch relationship,

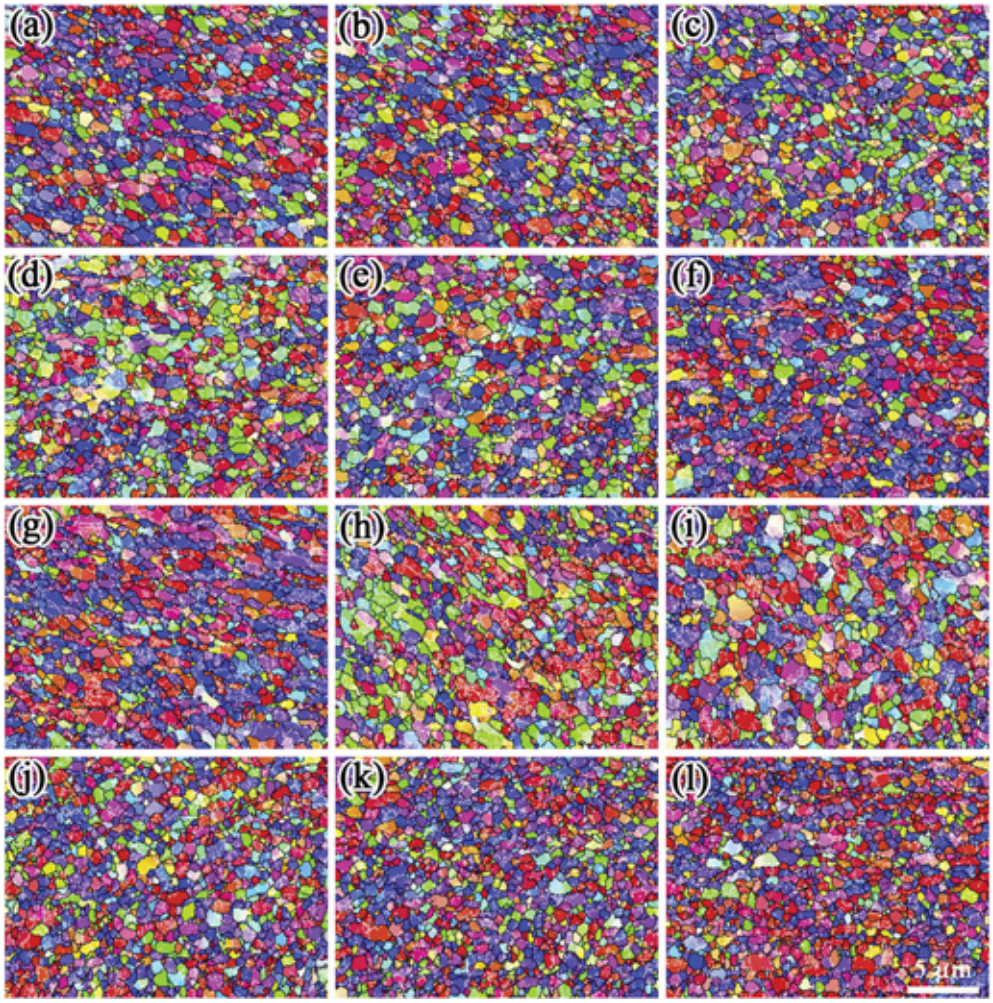

Fig. 4. EBSD microstructure of FSP-T3-b sample in the PZ (a-l: from top to bottom, along *z* direction in Fig. 1 with an interval of 120 nm).

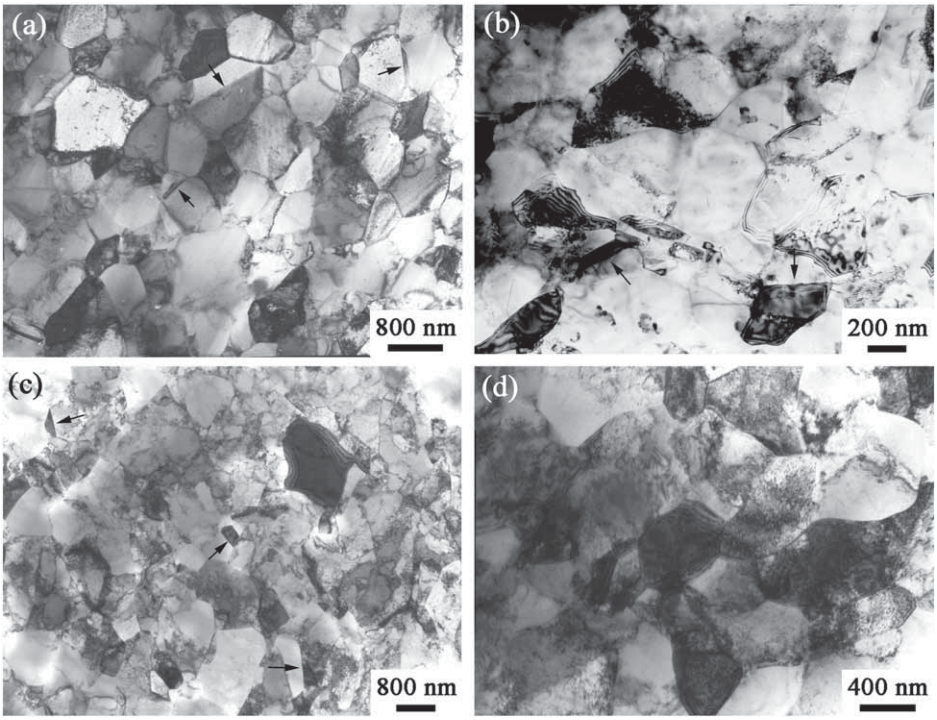

Fig. 5. TEM microstructure of FSP Cu with different parameters: (a) FSP-T3-a, (b) FSP-T3-b, (c) FSP-TU1-b, (d) FSP-TU1-c.

Table 1
The grain size and YS of FSP Cu under different heat input conditions.

Sample	Heat input condition	T3 Cu		TU1 Cu	
		Grain size (μm)	YS (MPa)	Grain size (μm)	YS (MPa)
a	400 rpm-20 mm shoulder	0.8	315	3	200
b	600 rpm-12 mm shoulder	0.5	460	0.8	300
c	400 rpm-10 mm shoulder	0.4	500	0.5	370

respectively. Chen et al. [27] summarized the relationship between the hardness and grain size of UFG Cu produced by different methods. The result indicated that the hardness data of UFG Cu still followed the Hall-Petch line extrapolated from the CG Cu even when the grain size was as small as 10 nm. However, for the UFG Cu samples prepared by SPD, the Hall-Petch line was obviously higher than that of the CG Cu, i.e., the hardness of SPD Cu was much higher than that predicted by the CG Cu Hall-Petch line due to the existence of dense dislocation walls, tangles, cells and non-equilibrium GBs [27]. For the FSP Cu, the relationship between the hardness and grain size was agreement well with the Hall-Petch relationship, which was slightly higher than the Hall-Petch boundary line of CG Cu, as shown in Fig. 9. It should be related to the weak texture and low dislocation density in FSP UFG Cu.

Fig. 10 shows the typical engineering tensile stress-strain curves of FSP T3 and TU1 UFG Cu with the same grain sizes of 800 nm and 500 nm, i.e., FSP-T3-a, FSP-T3-b, FSP-TU1-b, and FSP-TU1-c samples, respectively. It is clear that two Cu samples with different purities exhibited similar tensile behaviors, but the strength and ductility were lower in the FSP Cu with high purity. Compared with the CG Cu, the strength of the FSP UFG Cu was obviously improved, especially for the yield strength (YS), as shown in Table 1 and Fig. 10a and b. For the FSP-T3-a Cu, the YS was ~315 MPa and an uniform elongation (UE) of ~18% was achieved. For the FSP-TU1-b sample, similar tensile properties were obtained, but the YS slightly reduced to about 300 MPa with an UE of ~13%. Thus, under the suitable parameters, FSP can prepare UFG Cu with preferable strength-ductility synergy.

When the heat input was further reduced, the tensile strength of FSP-T3-b and FSP-TU1-c Cu reached to ~500 MPa and ~400 MPa, respectively. However, almost no UE was obtained, just like other SPD Cu. But the total elongation increased to about 30% and 20%, respectively, compared with that of the SPD Cu samples. From the true stress-strain curves of FSP Cu shown in Fig. 10c and d, obvious strain hardening was observed in FSP-T3-a and FSP-TU1-b samples. Moreover, even at very low heat inputs, FSP-T3-b and FSP-TU1-c samples did not exhibit fast plastic instability that usually occurred in SPD Cu samples. The stress was maintained at ~500 MPa and no strain softening occurred in FSP-T3-b Cu sample till a large strain of ~12% (Fig. 10c). For the FSP-TU1-c sample shown in Fig. 10d, strain hardening was observed till to a large stain of ~10%, showing an enhanced strain hardening capacity than that of the ECAP Cu with similar strength [28].

Fig. 11 shows the typical tension and compression true stress-strain curves of FSP-T3-a sample perpendicular and parallel to FSP direction, i.e. along *x* (transverse) and *y* (longitudinal) directions in Fig. 1, respectively. It is clear that four curves were almost the same till a large true strain of 0.25, indicating that isotropy and tension-compression symmetry were achieved in FSP Cu. Obviously, FSP Cu provides an ideal model material to investigate the intrinsic mechanical behaviors of the UFG materials.

Fig. 12 shows the relationship between YS and UE of several typical UFG Cu samples, it can be seen that most UFG Cu samples exhibited a high strength-low plasticity characteristic. Though very high YS was obtained in most SPD Cu samples, the UE was only ~2% [28–33]. However, FSP Cu samples and SPD Cu samples after annealing showed good strength-ductility synergy. Specially, the UFG Cu with a bimodal structure (designated as Bimodal-Cu in this study) prepared by Wang et al. [31] exhibited excellent strength-ductility synergy, which caught much attention. This Bimodal-Cu was prepared by SPD and annealing, where some micro-grains (1–3 μm) distributed in the UFG matrix. The existence of micro-grains increased the strain hardening in the

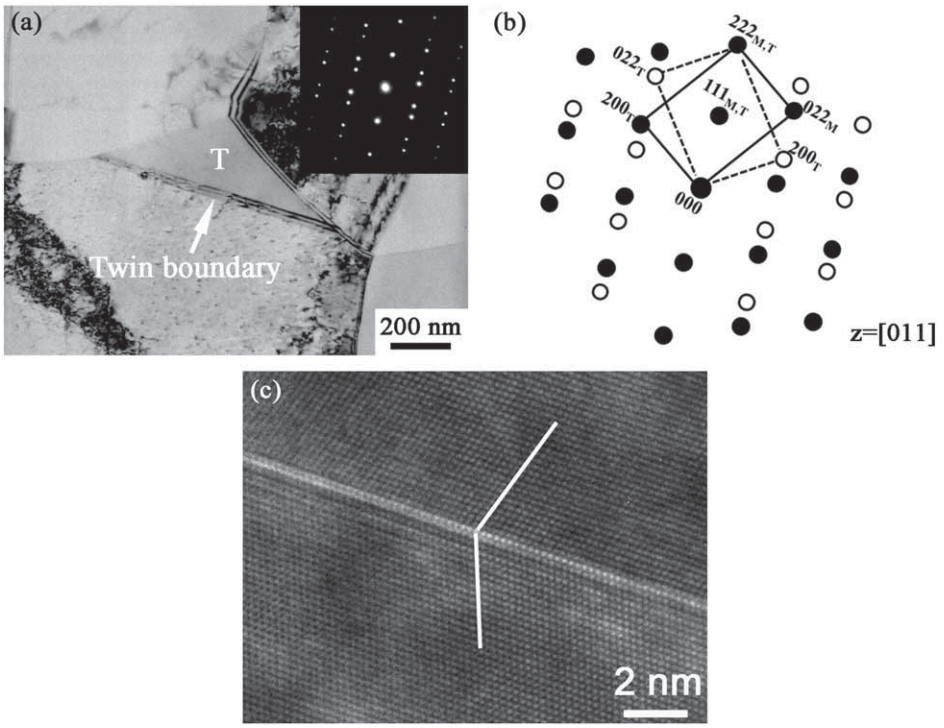

Fig. 6. Typical TEM images of TB in FSP-T3-a sample: (a) bright field image and selected-area election diffraction (SAED) pattern of TB, (b) the index of the SAD pattern, and (c) high-resolution TEM image of TB.

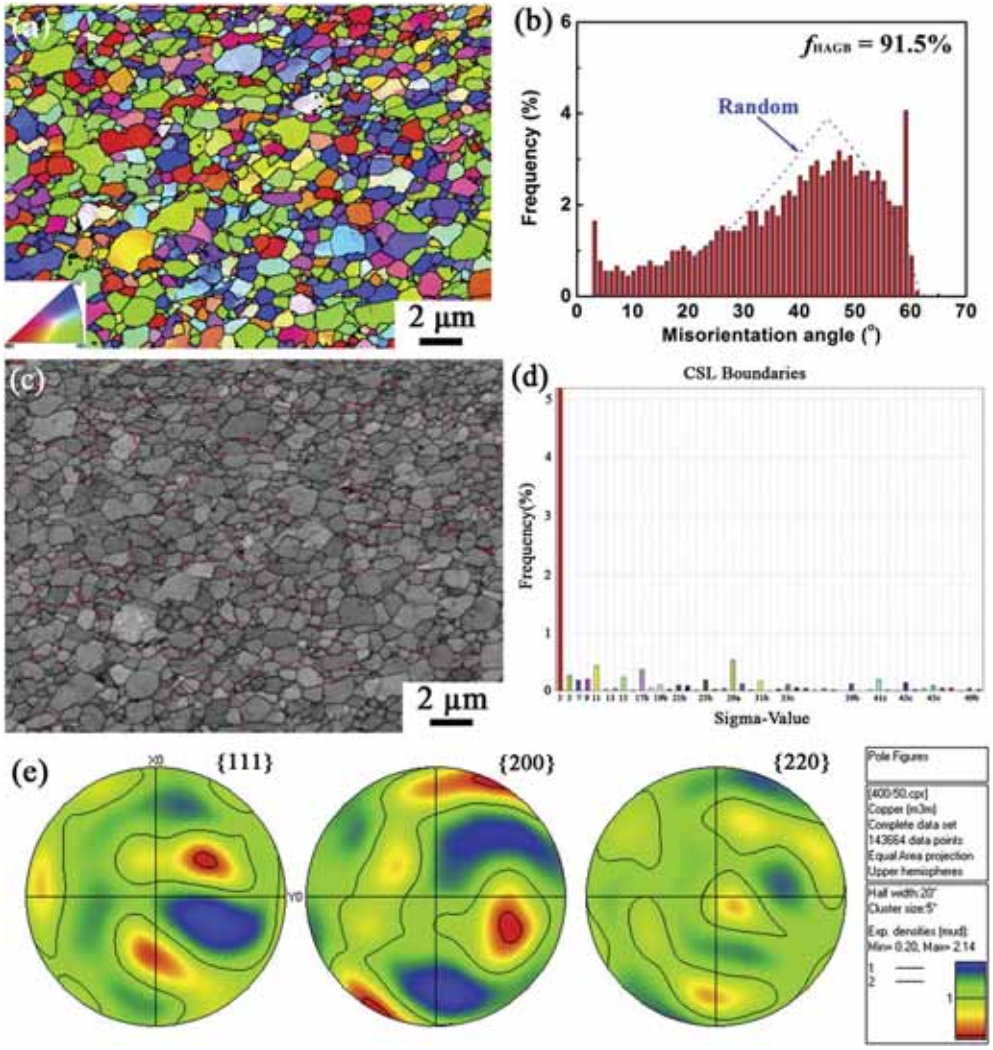

Fig. 7. EBSD results of FSP-T3-a sample: (a) EBSD image, distribution maps of (b) GB misorientation angle, (c) Σ3 TBs, (d) CSL GBs and (e) pole figures.

Bimodal-Cu, resulting in a high UE of ~30% together with relatively high YS of ~300 MPa.

However, it should be noted that the initial state of the BM has a significant effect on the strength and ductility of UFG Cu, which has been confirmed in the present study. Though a small gap existed in the YS of Cu samples with different purities, the UE showed very big differences in the Cu samples. When the YS of FSP Cu was about 300 MPa, the UE of both FSP Cu samples (FSP-T3-a and FSP-TU1-b) was about a half of their CG BMs. Moreover, the results of Wang et al. indicated that the UE of Bimodal-Cu was about 30%, which also reached half of the CG counterpart used in their study [31]. This means that the strength-ductility synergy of FSP UFG Cu was similar to that of Bimodal-Cu, which was obviously higher than that of traditional SPD Cu samples.

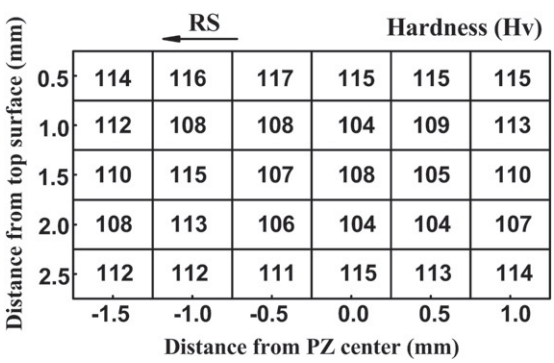

Fig. 8. Microhardness map of FSP-TU1-b sample.

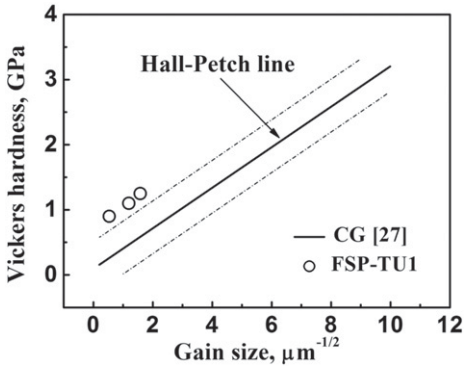

Fig. 9. Relationship of hardness and grain size of FSP-TU1 Cu.

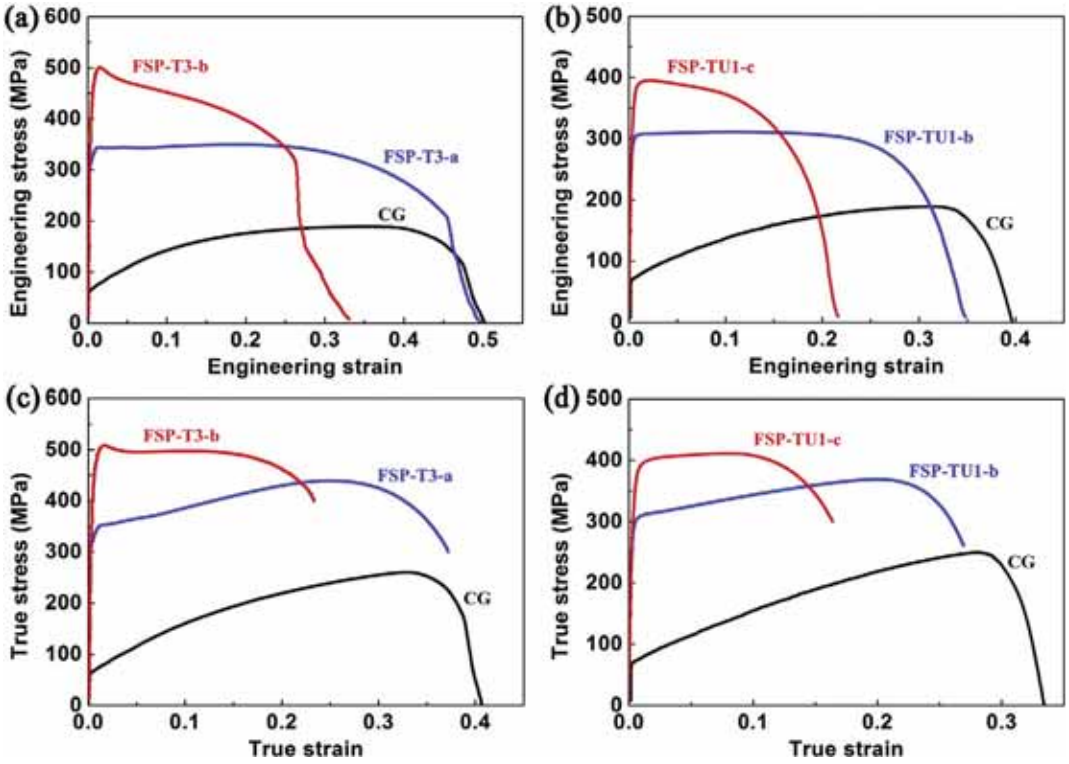

Fig. 10. Tensile curves of FSP Cu samples: engineering stress-stain curves of (a) T3 and (b) TU1 Cu, true stress-strain curves of (c) T3 and (d) TU1 Cu.

The strain hardening is very important for UFG materials because the onset of plastic instability in tension is governed by the Considére criterion:

$$\left(\frac{\partial\sigma}{\partial\varepsilon}\right)_{\dot{\varepsilon}} \leq \sigma \tag{1}$$

Where σ and ε are the true stress and true strain, respectively. The UFG material is easy to lose the strain hardening capacity during deformation due to their very low dislocation storage efficiency inside the tiny grains [4–6]. Therefore, very low ductility was achieved in most SPD UFG materials.

Zhao et al. [34] summarized the feasible strategies of improving the ductility of UFG materials. For pure metals, in addition to the introduction of high-density TBs through the electrolytic deposition (ED), reducing the dislocation density and increase the proportion of HAGBs are two effective methods to improve the ductility of the UFG material. Numerous studies confirmed that strength-ductility synergy could be enhanced clearly in the SPD Cu samples after annealing, though the strength decreased [29,31,33]. The enhanced ductility was due to the reduction of the dislocation density and the recrystallization process that introduced a certain amount of micron grains [29,31,33].

It is well accepted that FSP is a kind of thermo-mechanical process, which contains the combined effects of intense plastic deformation and annealing. Therefore, dynamic recovery and DRX process occurred during FSP [9,10], the dislocation density was very low in FSP UFG materials [11–17]. So, it provided more room to store dislocations during the tensile deformation process, which was beneficial to the improvement of the ductility of the UFG material. Moreover, the high fraction of HAGBs in FSP UFG Cu can also improve the strain hardening during tensile process, resulting in the enhanced ductility.

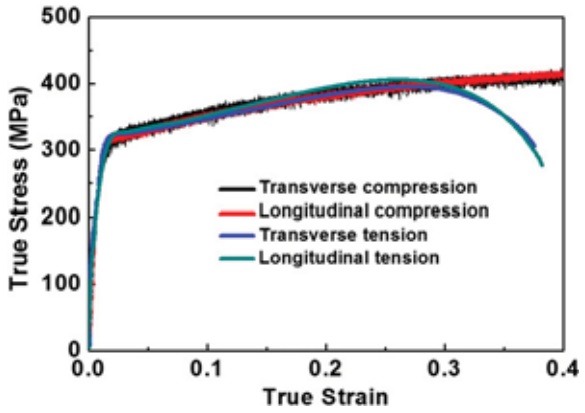

Fig. 11. Tension and compression curves of transverse and longitudinal direction (*x* and *z* directions in Fig. 1) in FSP-T3-a sample.

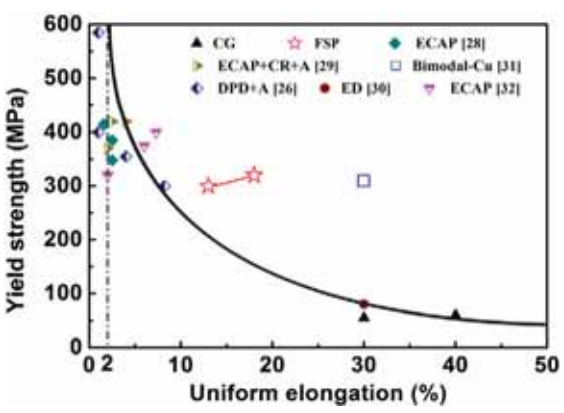

Fig. 12. Relationship of yield strength and uniform elongation of various UFG Cu samples prepared by FSP and other methods.

Obviously, the present study demonstrates that good strength-ductility synergy can be achieved in FSP UFG Cu. Moreover, it is reported that large-area bulk UFG materials with sound mechanical properties could be prepared by multiple-pass overlapping FSP method [35]. Therefore, FSP should be a potential method of preparing bulk UFG materials with good strength-ductility synergy in engineering applications.

4. Conclusions

In summary, the following conclusions are reached:

1. UFG pure Cu with uniform microstructure and good strength-ductility synergy was successfully prepared by FSP. Almost the same microstructure was observed at each area of the whole PZ and the fluctuation of the hardness value was very small. Moreover, isotropy and tension-compression symmetry were achieved in FSP Cu, which provided an ideal model material to investigate the intrinsic mechanical behavior of the UFG material.
2. The microstructure of the FSP Cu samples was characterized by equiaxed grains with low dislocation density and weak texture, and the fraction of the HAGBs was as high as ~91.5% in the FSP-T3-a Cu sample. Furthermore, many annealing TBs and other CSL GBs were frequently observed in the fine grains.
3. The relationship between the hardness and grain size of FSP UFG Cu was agreement with the Hall-Petch relationship, which was slightly higher than the Hall-Petch relationship boundary line of CG Cu. Enhanced strength-ductility synergy was achieved in the FSP UFG Cu, high UE of 18 and 13% with high YS of 315 MPa and 300 MPa were achieved in FSP-T3-a and FSP-TU1-b Cu samples, respectively. Further reducing the heat input, the YS increased to 460 MPa and 370 MPa in FSP-T3-b and FSP-TU1-c Cu samples, respectively, and the strain hardening capacity was higher than that of the SPD Cu.
4. The strength-ductility synergy in FSP Cu was comparable to that of the Bimodal-Cu prepared by SPD and annealing, and the good tensile properties were attributed to the enhanced strain hardening capacity in the special microstructure, where the dislocations could be accumulated effectively.

Acknowledgments

This work was supported by the National Natural Science Foundation of China under grant Nos. 51301178, and 51331008.

References

[1] R. Valiev, Nanostructuring of metals by severe plastic deformation for advanced properties, Nat. Mater. 3 (2004) 511–516.
[2] Y.T. Zhu, X.Z. Liao, Nanostructured metals - retaining ductility, Nat. Mater. 3 (2004) 351–352.
[3] N.R. Tao, K. Lu, Dynamic plastic deformation (DPD): a novel technique for synthesizing bulk nanostructured metals, J. Mater. Sci. Technol. 23 (2007) 771–774.
[4] A.P. Zhilyaev, T.G. Langdon, Using high-pressure torsion for metal processing: fundamentals and applications, Prog. Mater. Sci. 53 (2008) 893–979.
[5] R.Z. Valiev, R.K. Islamgaliev, I.V. Alexandrov, Bulk nanostructured materials from severe plastic deformation, Prog. Mater. Sci. 45 (2000) 103–189.
[6] A. Vinogradov, S. Hashimoto, V. Patlan, K. Kitagawa, Atomic force microscopic study on surface morphology of ultra-fine grained materials after tensile testing, Mater. Sci. Eng. A 319–321 (2001) 862–866.
[7] H. Mughrabi, H.W. Hoeppel, Cyclic deformation and fatigue properties of very fine-grained metals and alloys, Int. J. Fatigue 32 (2010) 1413–1427.
[8] R.S. Mishra, M.W. Mahoney, S.X. McFadden, N.A. Mara, A.K. Mukherjee, High strain rate superplasticity in a friction stir processed 7075 Al alloy, Scr. Mater. 42 (2000) 163–168.
[9] R.S. Mishra, Z.Y. Ma, Friction stir welding and processing, Mater. Sci. Eng. R 50 (2005) 1–78.
[10] Z.Y. Ma, Friction stir processing technology: a review, Metall. Mater. Trans. A 39 (2008) 642–658.
[11] P. Xue, Z.Y. Ma, Y. Komizo, H. Fujii, Achieving ultrafine-grained ferrite structure in friction stir processed weld metal, Mater. Lett. 162 (2016) 161–164.
[12] S. Meenia, F. Khan MD, S. Babu, R.J. Immanuel, S.K. Panigrahi, G.D.J. Ram, Particle refinement and fine-grain formation leading to enhanced mechanical behaviour in a hypo-eutectic Al-Si alloy subjected to multi-pass friction stir processing, Mater. Charact. 113 (2016) 134–143.
[13] P. Xue, B.L. Xiao, Z.Y. Ma, Achieving ultrafine-grained structure in a pure nickel by friction stir processing with additional cooling, Mater. Des. 56 (2014) 848–851.
[14] N. Xu, R. Ueji, Y. Morisada, H. Fujii, Modification of mechanical properties of friction stir welded Cu joint by additional liquid CO_2 cooling, Mater. Des. 56 (2014) 20–25.
[15] P. Xue, B.L. Xiao, Z.Y. Ma, Microstructure and mechanical properties of friction stir processed ultrafine-grained and nanostructured Cu-Al alloys, Acta Metall. Sin. 50 (2014) 245.
[16] C.I. Chang, X.H. Du, J.C. Huang, Achieving ultrafine grain size in Mg-Al-Zn alloy by friction stir processing, Scr. Mater. 57 (2007) 209–212.
[17] P. Xue, Z.Y. Huang, B.B. Wang, Y.Z. Tian, W.G. Wang, B.L. Xiao, Z.Y. Ma, Intrinsic high cycle fatigue behavior of ultrafine grained pure Cu with stable structure, Sci. China Mat. 59 (2016) 531–537.
[18] A. Orozco-Caballero, P. Hidalgo-Manrique, C.M. Cepeda-Jiménez, P. Rey, D. Verdera, O.A. Ruano, F. Carreño, Strategy for severe friction stir processing to obtain acute grain refinement of an Al-Zn-Mg-Cu alloy in three initial precipitation states, Mater. Charact. 112 (2016) 197–205.
[19] A. Heidarzadeh, T. Saeid, V. Klemm, Microstructure, texture, and mechanical properties of friction stir welded commercial brass alloy, Mater. Charact. 119 (2016) 84–91.
[20] Y.H. Zhao, J.F. Bingert, Y.T. Zhu, X.Z. Liao, R.Z. Valiev, Z. Horita, T.G. Langdon, Y.Z. Zhou, E.J. Lavernia, Tougher ultrafine grain Cu via high-angle grain boundaries and low dislocation density, Appl. Phys. Lett. 92 (2008) 081903.
[21] P. Xue, B.L. Xiao, Q. Zhang, Z.Y. Ma, Achieving friction stir welded pure copper joints with nearly equal strength to the parent metal via additional rapid cooling, Scr. Mater. 64 (2011) 1051–1054.
[22] Y.M. Yue, Z.W. Li, S.D. Ji, Y.X. Huang, Z.L. Zhou, Effect of reverse-threaded pin on mechanical properties of friction stir lap welded alclad 2024 aluminum alloy, J. Mater. Sci. Technol. 32 (2016) 671–675.
[23] J. Kang, J.C. Li, Z.C. Feng, G.S. Zou, G.Q. Wang, A.P. Wu, Investigation on mechanical and stress corrosion cracking properties of weakness zone in friction stir welded 2219-T8 Al alloy, Acta Metall. Sin. 52 (2016) 60–70.
[24] P. Xue, B.L. Xiao, Z.Y. Ma, High tensile ductility via enhanced strain hardening in ultrafine-grained Cu, Mater. Sci. Eng. A 532 (2012) 106–110.
[25] P. Xue, B.L. Xiao, Z.Y. Ma, Enhanced strength and ductility of friction stir processed Cu-Al alloys with abundant twin boundaries, Scr. Mater. 68 (2013) 751–754.
[26] C.X. Huang, H.J. Yang, S.D. Wu, Z.F. Zhang, Microstructural characterization of Cu processed by ECAP from 4 to 24 passes, Mater. Sci. Forum 584–586 (2008) 333–337.
[27] J. Chen, L. Lu, K. Lu, Hardness and strain rate sensitivity of nanocrystalline Cu, Scr. Mater. 54 (2006) 1913–1918.
[28] F.D. Torre, R. Lapovok, J. Sandlin, P.F. Thomson, C.H.J. Davies, E.V. Pereloma, Microstructures and properties of copper processed by equal angular extrusion for 1–16 passes, Acta Mater. 52 (2004) 4819–4832.
[29] Y.M. Wang, E. Ma, M.W. Chen, Enhanced tensile ductility and toughness in nanostructured Cu, Appl. Phys. Lett. 80 (2002) 2395–2397.
[30] L. Lu, L.B. Wang, B.Z. Ding, K. Lu, High-tensile ductility in nanocrystalline copper, J. Mater. Res. 15 (2000) 270–273.
[31] Y.M. Wang, M.W. Chen, F.H. Zhou, E. Ma, High tensile ductility in a nanostructured metal, Nature 419 (2002) 912–915.
[32] R.Z. Valiev, I.V. Alexandrov, Y.T. Zhu, T.C. Lowe, Paradox of strength and ductility in metals processed by severe plastic deformation, J. Mater. Res. 17 (2002) 5–8.
[33] Y.S. Li, Y. Zhang, N.R. Tao, K. Lu, Effect of thermal annealing on mechanical properties of a nanostructured copper prepared by means of dynamic plastic deformation, Scr. Mater. 59 (2008) 475–478.
[34] Y.H. Zhao, Y.T. Zhu, E.J. Lavernia, Strategies for improving tensile ductility of bulk nanostructured materials, Adv. Eng. Mater. 12 (2010) 769–778.
[35] P. Xue, B.L. Xiao, Z.Y. Ma, Achieving large-area bulk ultrafine grained Cu via submerged multiple-pass friction stir processing, J. Mater. Sci. Technol. 29 (2013) 1111–1115.